Composite Structures 168 (2017) 26–32

Contents lists available at ScienceDirect

Composite Structures

journal homepage: www.elsevier.com/locate/compstruct

Young's modulus estimation for CNT reinforced metallic foams obtained using different space holder particles

L. Pérez [a], R. Mercado [a], I. Alfonso [b,*]

[a] Department of Mechanical Engineering, Universidad Técnica Federico Santa María, Av. España 1680, Casilla 110-V, Valparaíso, Chile
[b] Instituto de Investigaciones en Materiales, Unidad Morelia, Universidad Nacional Autónoma de México, Campus Morelia UNAM. Antigua Carretera a Pátzcuaro No. 8701, Col. Ex-Hacienda de San José de la Huerta, CP. 58190 Morelia, Michoacán, Mexico

ARTICLE INFO

Article history:
Received 18 October 2016
Revised 12 December 2016
Accepted 2 February 2017
Available online 8 February 2017

Keywords:
Foam
Composite
FEA
DEM
CNT

ABSTRACT

In this work Finite Element Analysis (FEA) was used in order to estimate the effect of the pore size and the volume fraction of carbon nanotubes (CNT) used as reinforcement, for Al-12%Si foams with 50% of porosity. Two different space holder particles (SHP) were used to simulate foams manufactured by infiltration, modeling pores of two different fractal distributions according to the size of the SHPs: NaCl and NH_4HCO_3. Random pore arrangements were modeled combining Discrete Element Method (DEM) and FEA. Coordinates were firstly generated using DEM, while in a second stage CNTs and pores were modeled by FEA. Estimations show important differences according to the used SHP, decreasing the Young's modulus for the foams with the smallest pore sizes. The Young's modulus also increased with the CNT volume fraction. Results showed the importance of the selection of random models and the use of FEA for predicting the Young's modulus of reinforced metallic foams.

1. Introduction

Modern world needs new advanced materials with unique combination of properties that allow new applications. Metallic foams are among these new class of materials which prime advantage is their excellent combination of good mechanical properties and low weight [1,2]. They show several properties such as high strength-to-weight ratio, high energy absorption capacity, large specific surface, high gas and liquid permeability, and low thermal conductivity. Among other applications, these materials have been used as impact absorbers, dust and fluid filters, heat exchangers and flame arresters [1,2]. The final properties of a foam highly depend on its structure, being among the most important parameters pore size and distribution, and thickness of the cell walls [3]. In order to optimize the design process, it is very important to have predictions of their mechanical behavior before their fabrication. This necessity increases when the foam is reinforced for improving the mechanical properties, because the final properties will not only depend on the pores but also on the reinforcement. However, there are limitations in terms of the degree of concentration of the secondary phase (in this case pores and reinforcements) that can be dispersed into the primary phase and the degree of interconnectivity between these phases. For metallic matrices, as is the case of metallic foams, CNTs are one of the newest used reinforcements. They provide lightweight and high mechanical and thermal properties to the metal matrix composites (MMC), being Al and Mg foams among the most commonly studied [4–6]. One of the manufacturing methods for metallic foams, including foams with CNTs, is the infiltration process incorporating removable Space Holder Particles (SHP) as pre-forms, followed by their dissolution [7,8]. For the foams manufactured using this method it is possible to predict the pore size according to the size of the space holder [9]. Due to its modeling capability, Finite Element Analysis (FEA) is one of the methods used to predict the mechanical properties of heterogeneous materials, such as foams and composites, being able to model different geometries, including both the pores and the reinforcements, and analyze their effect on the mechanical properties of the material [5,9–12]. Theoretical models are not available for estimating the elastic properties of fiber reinforced foams, and a simulation study is a very important way to insight into the properties of these materials. The validity of such predictions mainly depends on the proximity of the model to the real foam topology, because in real cellular structures, foam topology is typically aperiodic, non-uniform and disordered. Some works have modeled the porosity using random arrangements for the pores [9,13], being more realistic and recommended for foams obtained by infiltration or powder metallurgy, where the porosity highly depends on the space holder. In these works the position of the pores is first generated into a container, controlling then their shapes (e.g. spheres),

* Corresponding author.
E-mail address: ialfonso@unam.mx (I. Alfonso).

http://dx.doi.org/10.1016/j.compstruct.2017.02.017
0263-8223/

sizes, and the distance between their centers in order to control interconnectivity; while in a third stage the pores are generated by deleting the volume of the resulting geometries from the container volume. Discrete Element Method (DEM) is one of the techniques that has been used for generating these random positions due to its ability for modeling the behavior of particulate systems [14]. These kind of procedures for the generation of the position of the pores can be also used for generating the location of random arranged reinforcements, and there is some work in literature dealing mainly with the effect of their percentage on the mechanical properties of the composites [15,16]. About reinforced metallic foams, few works study the dual effect of pores and reinforcements on the mechanical properties of these materials [5,17,18]. There are two important works by Frantziskonis [19,20] related to the relevant size of pores and particles for different materials, focused to analyze the role of each of these microstructures on different properties. These works used the wavelet transform as a mathematical microscope, and report that the importance (contribution) of each microstructural feature is highly dependent of factors such as the porosity scale and the distance between pores. Based on the above, and due to the importance of optimization for the design process, the first objective of the present work is to analyze the effect of CNTs and pores on the mechanical properties of reinforced metallic foams. In order to achieve this objective there were obtained two kind of randomly arranged models: one for MMCs with a Al-12%Si matrix and different percentages of CNTs, and the other one simulating foams obtained infiltrating these MMCs using two different SHP. The models as well as the predictions derived from them will provide important information for the design and further fabrication of these materials according to the use requirements.

2. Modeling and simulation

In this work the elastic behavior of foams reinforced with CNTs was estimated through DEM-FEA models divided into two parts: i) models of MMCs consisting on a Al-12%Si matrix and five different volume fractions of CNTs as reinforcement; and ii) models of the Al-12%Si foams with 50% of porosity and two different pore size distributions according to the used SHP (NaCl and NH_4HCO_3), as will be further analyzed. In a first stage of the simulation the elastic behavior of the MMC models was estimated using FEA. Then, in a second stage, the predictions derived from the MMC models were used as input parameters for the simulation of the foams. This procedure allows the study of a complex dual heterogeneous material (pores and reinforcements) into two more simple models. Only using these combined models it is possible to study this kind of problem, because it is reported that yet, even with modern computers capable of handling a large number of finite elements, it becomes practically impossible to simulate a reasonable size of the material because of the multiscale nature of the problem [19]. Detailed explanations about models and simulations are included below.

2.1. Generation of random distributions using DEM

Open source DEM simulation software LIGGGHTS® [21] was used in order to generate randomly distributed coordinates for pores and CNTs location, being the initial stage of the modeling process. This first step consists on ascertaining the behavior of spherical particles immersed into cylinders. The cylinders used for generating the coordinates where 100 μm in diameter and 192 μm in height for the case of foams using NaCl as SHP; 50 μm in diameter and 96 μm in height for the case of NH_4HCO_3; and 5 μm in diameter and 5.75 μm in height for the MMCs. The used criterion for selecting the size of the cylinders was the needed for computations convergence already studied in a previous work [9], i.e. the representative volume elements (RVE) must be at least ~ 2.5–3.5 times the maximum size of certain feature that represents the material. In our case these features are cells including pores or CNTs. Depending on the porosity percentage or the CNT volume fraction certain number of spheres was inserted. The conditions for the interactions between these inserted particles were selected just for generating a high interaction between particles and to get the desired random distribution. In order to obtain repetitive results three random distributions were obtained for each model for CNTs and foams, reporting as Young's modulus the average obtained using these distributions.

2.2. Finite elements models for the MMCs

Once the coordinates were obtained, these results were post-processed in order to generate two kind of scripts using commercial FEA software ANSYS 14.5, locating the pores in one script and the CNTs in the other script, followed by the creation of CAD models. CNTs were located at the generated coordinates modeled as solid cylinders of 0.064 μm in diameter and 1 μm in height, being the aspect ratio 15.6 (L/D = 1000/64 nm) [10]. The measured volume fractions for the inserted CNTs ranged from 0.003 to 0.022. These small quantities were selected in order to optimize the computational requirements. Fig. 1a-c shows the modeled cylindrical specimens with three different CNT volume fractions, engendered through DEM-FEA combination. As can be observed, the distributions of the CNTs are random. Their directions were obtained through the generation of three random angles for obtaining each *x*, *y* and *z* direction.

2.3. Finite elements models for the foams

As for the MMC models, the FEA models of the foams also used the scripts obtained through DEM for locating the pores. The size of the pores were selected according to the observed in a previous work [9], where it was demonstrated that the size of the pores for foams obtained by powder metallurgy using the dissolution and sintering process highly depends on the space holder particle. This behavior is also expected for foams obtained using infiltration. This previous work also showed that the use of a reduced fractal approach for the porosity distribution gives excellent estimations. Taking these results into account, pores were modeled as spheres and following fractal distributions including 4 pores of 10 μm per each pore of 20 μm for pores obtained using NaCl as SHP, and 2 pores of 5 μm per each pore of 10 μm when NH_4HCO_3 was the SHP. These distributions were selected according to experimental observations revealing that for NH_4HCO_3 particles the ratio between the logarithms of the relative sizes and quantities for big and small particles was 1.0. This value corresponds to the fractal dimension (d_f) of the distribution of these particles. According to a previous work [9] the distribution of the pores obtained using NaCl as SHP agrees with the distribution of NaCl particles, being both fractals, with d_f values of 1.95 and 2.0, respectively. Fig. 2a-b shows the modeled cylindrical specimens for the foams with porosities of 50% and the two different pore size distributions. It is worth mentioning that the interconnection between the pores observed for the models in Figs. 2a and 2b favors Young's moduli predictions closer to the real values.

2.4. Simulation for the MMCs

The Young's moduli of the MMCs with different CNT volume fractions were uni-axially estimated when applying equivalent compressive displacements on the nodes of the upper end of the cylindrical specimens. The Al-12%Si matrix used in this work for

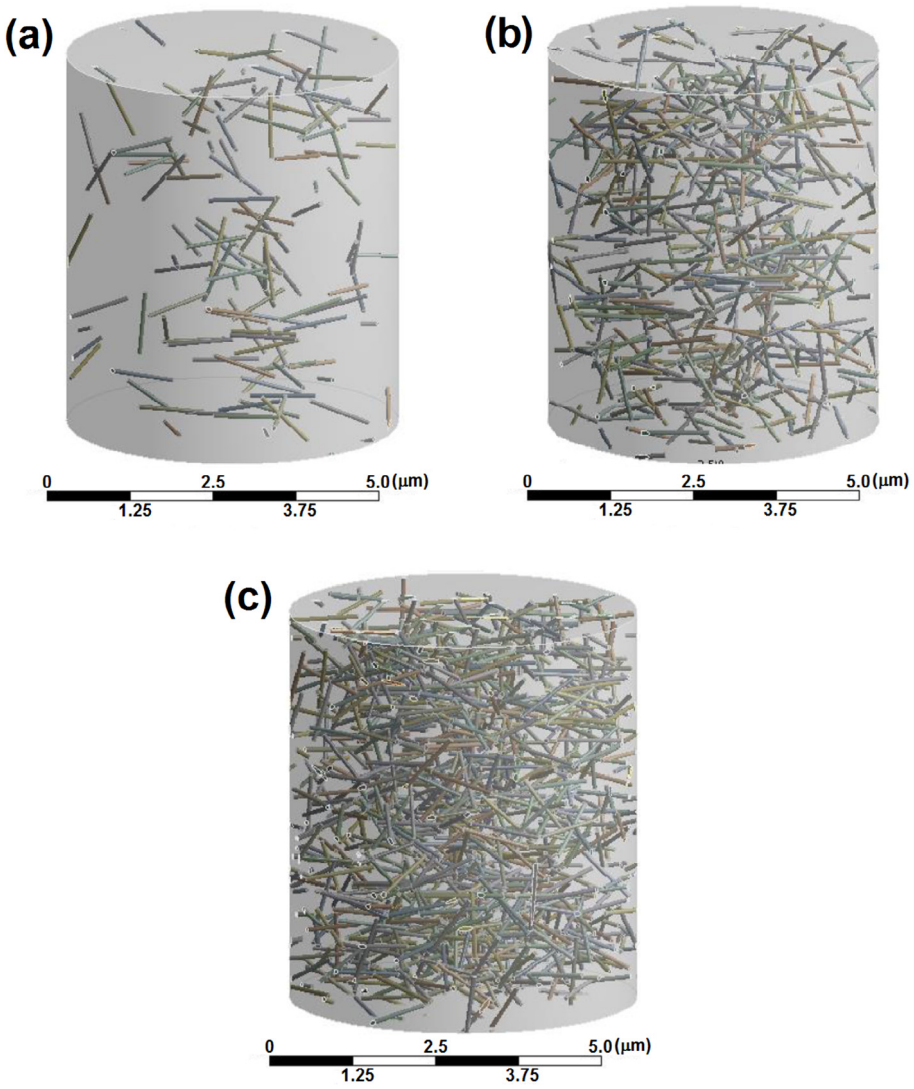

Fig. 1. FEA models of MMCs reinforced with volume fractions of randomly ordered CNTs of: (a) 0.003, (b) 0.011, and (c) 0.022.

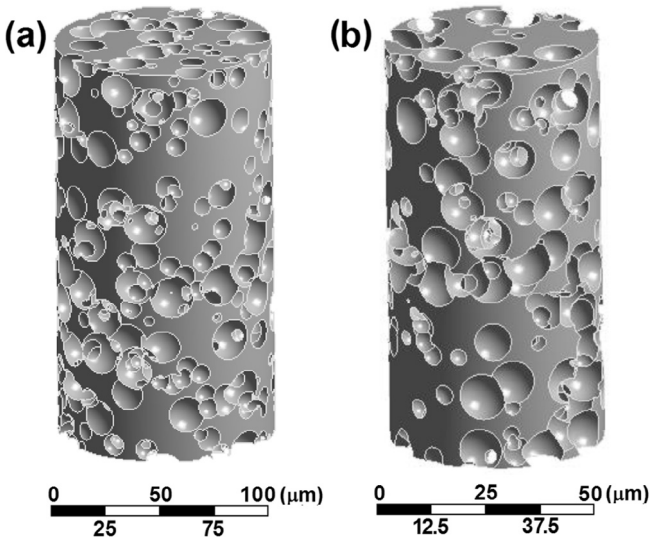

Fig. 2. FEA models of foams with porosities of 50% and pore size distributions of: (a) 4 pores of 10 μm per each pore of 20 μm, and (b) 2 pores of 5 μm per each pore of 10 μm.

simulating purposes has been used for CNT reinforced MMCs, as the work of Joshi et al. [15] obtained using a squeeze casting process, and has a typical Young's modulus of 77 GPa, and a Poisson coefficient of 0.33. The CNTs were modeled using a Young's modulus close to 680 GPa, and Poisson's ratio of 0.27 [10]. The SOLID187 3-D 10-node tetrahedral structural solid element was employed for meshing. The number of nodes ranged from 5 to 31×10^5, while the number of elements from 2.3 to 15×10^5, increasing these quantities with the increase in the CNT volume fraction. The coupled-node boundary condition (keeping the nodes in the same plane) was used for the upper face of the cylinder. Fig. 3a shows the meshed model for a MMC reinforced with a CNT volume fraction of 0.011. As can be observed, smaller elements (circled) were used to ensure the connectivity between matrix and CNTs. The meshed model for an isolated CNT can be observed in Fig. 3b, being a usual mesh for these cylindrical or tubular structures.

Young's modulus can be obtained from the response of the simulated compression test, and along the z-axis (E_z), it can be determined by:

$$E_z = \frac{\sigma_z}{\varepsilon_z} \tag{1}$$

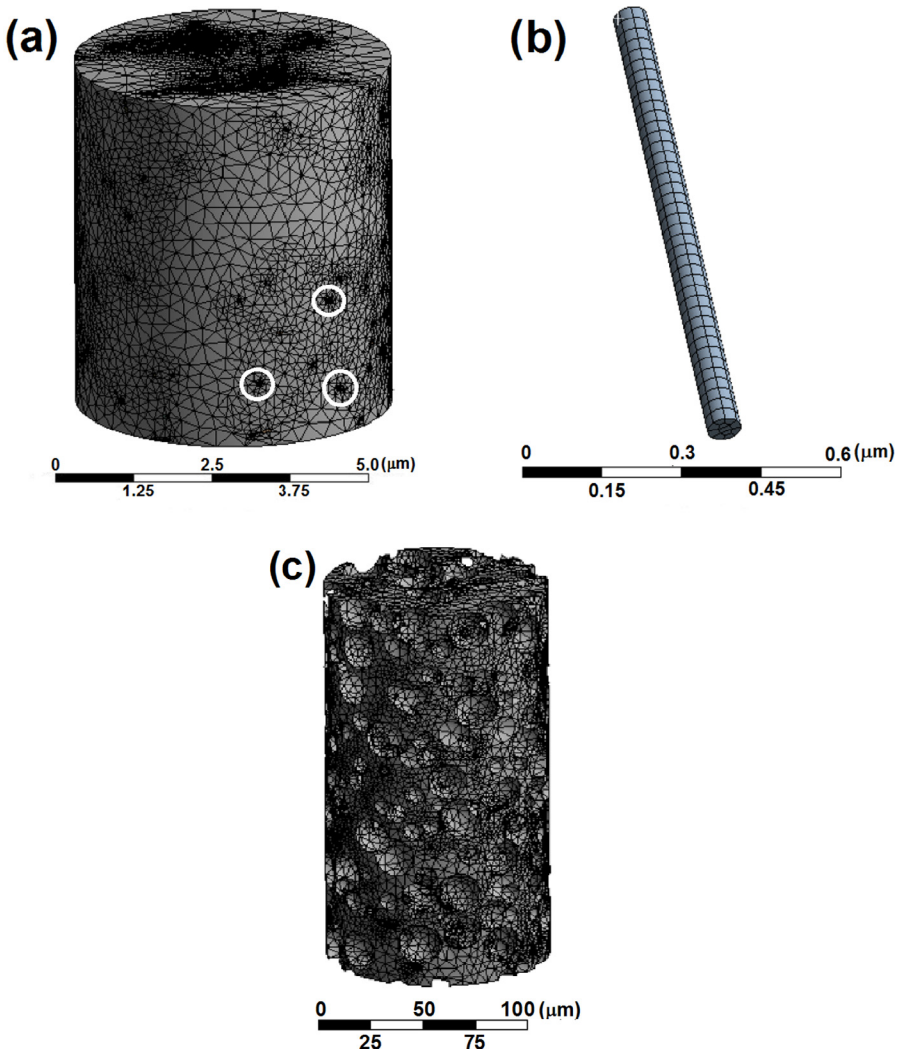

Fig. 3. Meshing for: (a) MMC reinforced with 0.011 volume fraction of CNTs (intersections circled); (b) an isolated CNT; and (c) foam with 50% of pores of 10–20 μm.

where σ_z and ε_z are the stress and the strain in *z*-axis, respectively. The displacement applied (0.1 μm) to the cylinder in z-axis (u_z) is used for the strain determination:

$$\varepsilon_z = \frac{u_z}{L_z} \tag{2}$$

where L_z is the original height of the cylindrical specimen. The stress necessary for solving Eq. (1) is determined using the following equation:

$$\sigma_z = \frac{F_Z}{A} \tag{3}$$

where F_z is the reaction force in the z-axis obtained through the FEA simulation, for the nodes of the bottom end of the cylindrical specimens; while *A* is the area of this surface.

2.5. Simulation for the foams

The Young's moduli of the foams with 50% of porosity and different pore sizes were determined using the same procedure already explained in Section 2.3 for the MMCs. For this case the displacements for Eq. (2) were 5 μm and 10 μm for the cylindrical models with heights of 96 and 192 μm, respectively. The Young's moduli used for the solid part of the foams were the obtained after the simulation of the MMCs, and depended on the volume fraction of CNTs. In this case, the most important difference was the use of the effective area (A_e) in Eq. (3), which is the flat area (without holes produced by the pores), being the section which reacts to the applied stress. The number of nodes for these cases ranged from 3.8 and 7.9×10^5, while the number of elements was between 2.4 and 5×10^5. The advantage of using the combined models could be resumed comparing this quantity of elements to the total elements that could be obtained if the foams were modeled including CNTs in only one model, reaching 12×10^8, quantity that is three orders of magnitude higher than the used in the combined model. This quantity of elements hinders the simulation process due to it requires an increased amount of computational resources. Fig. 3c shows the meshed model for the foams with pores of 10–20 μm. In order to establish the limits for the use of this combined analysis, it is important to measure the average distance between pores, i.e. the size of the cell walls. As was already mentioned, there is a condition establishing that the representative volume elements (RVE) must be at least ~ 2.5–3.5 times the maximum size of certain feature that represents the material. This condition should be also taken into account for the cell walls included into the models, which sizes should be at least equivalent to the length of 2.5–3.5 CNTs. The use of this criterion agrees with the work of Frantziskonis [19], who demonstrated that for Al alloys with pores and inclusions the autocorrelation distance (equivalent to cell wall distance, *cw*) plays a very relevant role. Frantziskonis

found that for small values of *cw* (case I) the inclusions had a dominant effect, while when *cw* increased (case II) the pores were dominant. Case I is similar to a model were the size of the cell walls is lower than the length of 2.5–3.5 CNTs, and the predominant effect of the CNTs origins the over prediction of mechanical properties. Otherwise, case II could be compared to a model with cell walls containing much more CNTs, fact that favors predictions closer to the real values. Now, the mean cell wall size (*cw*) is proportional to the porosity percentage and the size of the pores, as in the case of the inter-particle spacing, which is defined as the distance from the surface of one particle to that of another, as follows [22]:

$$cw = d\frac{(1-f)}{f} \tag{4}$$

where f is the particle volume fraction, and d the average particle diameter. For a porosity of 50%, if we use the pore diameter as d, and f as the fraction of the porosity, resulting cell wall sizes are 12 μm for the foams with 4 pores of 10 μm per each pore of 20 μm, and 6.67 μm for the foams with 2 pores of 5 μm per each pore of 10 μm. As CNTs were modeled as solid cylinders of 1 μm in height, the condition is fulfilled due to the enough size of the cell walls. This condition is also fulfilled for porosities as high as ~70% (cell walls of 5.14 and 2.86 μm, respectively).

3. Results and discussion

The graphical response of the models to the total applied displacements for a Al-12%Si matrix reinforced with a CNT volume fraction of 0.011 MMC, and for a foam with 50% of porosity and pores of 10–20 μm (without reinforcement) can be observed in Fig. 4a and 4b, respectively. These figures show the distributions of the directional displacements in *z*, and as expected, the maxima are for the nodes of the upper end of the cylindrical specimens. The images were similar for the models of the reinforced foams, just changing the reaction forces, data that can be observed in Table 1.

The values of the Young's moduli were determined after processing these results.

Fig. 5a shows the strengthening effect of the CNT on the elastic behavior of the MMCs, also comparing with maximum and minimum results for conventional Rule of Mixtures. For MMCs reinforced with ordered fibers, the equation for Rule of Mixtures when the stress is parallel to the axis of the reinforcement is as follows [10]:

$$E_L = E_m(1-f_R) + E_R f_R \tag{5}$$

where E_m is the Young's modulus for the matrix; while E_R and f_R are, respectively, the Young's modulus and the volume fraction for the reinforcement. Otherwise, the equation for a transversal stress is as follows:

$$E_T = E_m E_R/(E_R f_m + E_m f_R) \tag{6}$$

As can be observed in Fig. 5a, the increase in the Young's modulus estimated using FEA is between maxima and minima values predicted by the Rule of Mixtures, fact that demonstrates the efficacy of the FEA predictions for the MMCs. Other works have shown that experimental results are generally located between maxima and minima values predicted using Rule of Mixtures or other models [10,23].

On the other hand, Fig. 5b shows the effect of the CNT volume fraction on the elastic behavior of the foams with 50% of porosity and pores produced by the use of NH_4HCO_3 and NaCl as space holders. Comparing first the Young's modulus of the bulk Al-12% Si matrix and the foams it can be observed that the porosity lead to important decreases, diminishing from 77 GPa for the bulk material to 32 GPa and 36 GPa for the foams with pores of 5–10 μm and 10–20 μm, respectively. The lower value obtained for the foam with pores of 5–10 μm could be explained due to the fact that when comparing foams with the same porosity the smaller the pores the smaller the cell-wall thickness, leading to lower values of the Young's modulus. This result agrees well with

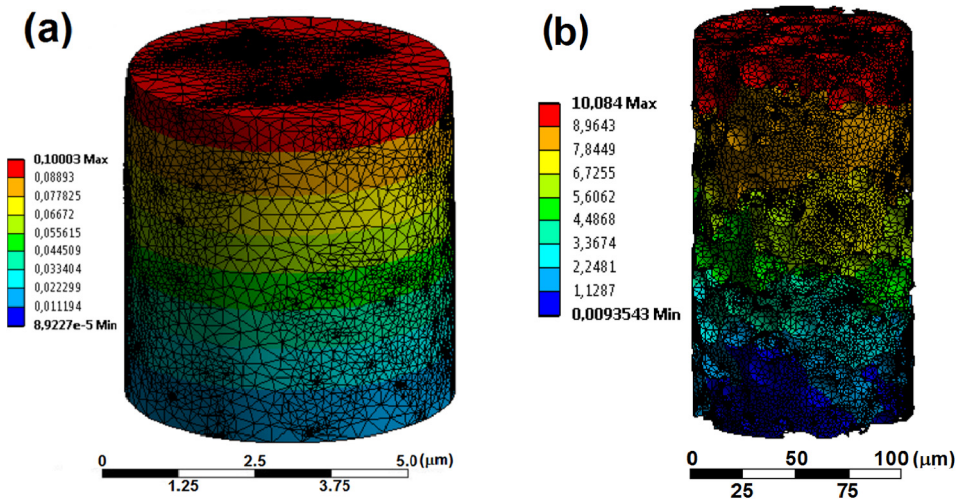

Fig. 4. Directional displacement in *z* under compression for a: (a) MMC reinforced with a volume fraction of randomly ordered CNTs of 0.011, and (b) a Al foam with 50% of porosity and pores of 10–20 μm

Table 1
Reaction forces (in N) obtained for the models of the CNT reinforced MMCs, the foams, and the foams reinforced with CNTs ($\times 10^{10}$ for the MMCs, and $\times 10^{12}$ for the foams).

	CNT volume fraction					
	0	0.003	0.006	0.011	0.017	0.022
MMCs		2.725	2.742	2.766	2.796	2.814
Foam, pores 5–10 μm with CNTs	1.800	1.864	1.877	1.893	1.914	1.926
Foam, pores 10–20 μm with CNTs	0.710	0.737	0.744	0.748	0.757	0.762

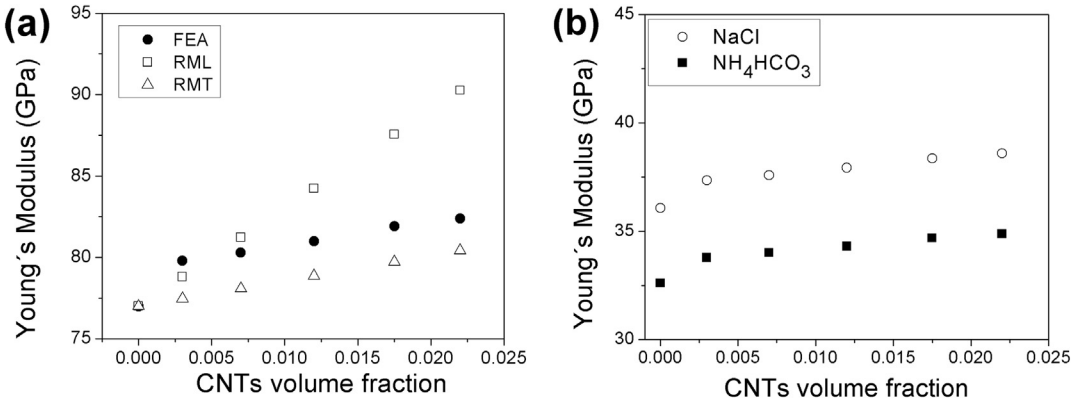

Fig. 5. Compressive Young's modulus variation depending on the CNT volume fraction for: (a) Al-12%Si matrix MMCs, and (b) foams with porosities of 50% obtained using NaCl and NH_4HCO_3 as space holders. For the MMCs the Young's moduli for longitudinal (RML) and transversal (RMT) Rule of mixtures were inserted in (*a*).

the experimentally observed by Figueroa et al. for Mg foams with porosities of 70% and different pore sizes [24]. Related to the comparative reinforcement effect of the CNTs it can be observed that for the two foams the increase in the Young's moduli are similar. In both cases CNT volume fractions increments as low as 0.022 lead to Young's moduli increases of ~7%.

These results showed the importance of the DEM-FEA combination for the study of both composites and foams. The use of DEM in an initial stage allowed taking into account the random distribution of reinforcements and pores. The combination of the two independent models (first for MMCs and then for foams with MMC matrices) helped to predict by FEA in an easier and rather accurate way the elastic compressive behavior of these materials.

4. Conclusions

After the analysis of the estimated Young's moduli for the foams reinforced with CNTs, the following can be concluded:

- DEM demonstrated to be an excellent tool for generating the location of heterogeneities randomly distributed in materials.
- The introduction of random models generated using a DEM–FEA combination made it possible to realize a more realistic topology of CNT reinforced composites and foams.
- It was demonstrated the efficacy of the procedure introduced in this work, using the FEA previously predicted Young's moduli for the MMCs as input data for estimating the elastic behavior of CNT reinforced foams.
- For both, Rule of Mixtures and FEA models, the elastic moduli of the MMCs significantly linearly increased as the CNT volume fraction increases. The estimations obtained using FEA were between maxima and minima values obtained using the Rule of Mixtures.
- FEA estimations showed that the selection of the size of the pores depending on the used space holder play an important role in the elastic behavior of the metallic foams. For foams with the same porosity, smaller pores lead to lower values of elastic moduli.

Acknowledgements

The authors would like to acknowledge the financial support from UNAM PAPIIT IN117316 for funding the project. L. Pérez acknowledges the financial support from the Advanced Center for Electrical and Electronic Engineering, AC3E, Basal Project FB0008, CONICYT.

References

[1] Banhart J, Ashby MF, Fleck NA. Metal foams and porous metal structures. Bremen: Verlag MIT Publishing; 1997.
[2] Gibson LJ, Ashby MF. Cellular solids: structure and properties. 2nd ed. Cambridge: Cambridge University Press; 1997.
[3] Davies GJ, Zhen S. Metallic foams: their production, properties and applications. J Mater Sci 1983;18:1899. http://dx.doi.org/10.1007/BF00554981.
[4] He CN, Zhao NQ, Shi CS, Song SZ. Fabrication of aluminum carbide nanowires by a nano-template reaction. Carbon 2010;48(4):931–8. http://dx.doi.org/10.1016/j.carbon.2009.10.004.
[5] Duarte I, Ventura E, Olhero S, Ferreira JMF. An effective approach to reinforced closed-cell Al-alloy foams with multiwalled carbon nanotubes. Carbon 2015;95:589–600. http://dx.doi.org/10.1016/j.carbon.2015.08.065.
[6] Li Q. Effect of porosity and carbon composition on pore microstructure of magnesium/carbon nanotube composite foams. Mater Des 2016;89:978–87. http://dx.doi.org/10.1016/j.matdes.2015.09.134.
[7] Ashby MF, Evans AG, Fleck NA, Gibson LJ, Hutchinson JW, Wadley HNG. Metal foams: a design guide. USA: Butterworth-Heinemann; 2000.
[8] Banhart J. Manufacture, characterisation and application of cellular metals and metal foams. Prog Mater Sci 2001;46:559. http://dx.doi.org/10.1016/S0079-6425(00)00002-5.
[9] Pérez L, Aguilar C, Lascano S, Domancic D, Alfonso I. Simplified fractal FEA model for the estimation of the Young's Modulus of metallic foams obtained by powder metallurgy: validation for Ti foams. Mater Des 2015;83:276–83. http://dx.doi.org/10.1016/j.matdes.2015.06.038.
[10] Alfonso I, Navarro O, Vargas J, Beltrán A, Aguilar C, González G, et al. FEA evaluation of the Al_4C_3 formation effect on the Young's modulus of carbon nanotube reinforced aluminum matrix composites. Compos Struct 2016;127:420–5. http://dx.doi.org/10.1016/j.compstruct.2015.03.032.
[11] Antunes FV, Ferreira JAM, Capela C. Numerical modelling of the Young's modulus of syntactic foams. Finite Elem Anal Des 2011;47:78–84. http://dx.doi.org/10.1016/j.finel.2010.09.007.
[12] Jhaver R, Tippur H. Processing, compression response and finite element modeling of syntactic foam based interpenetrating phase composite (IPC). Mater Sci Eng A-Struct 2009;499:507–17. http://dx.doi.org/10.1016/j.msea.2008.09.042.
[13] Kırca M, Gul A, Ekinci E, Yardım F, Mugan A. Computational modeling of micro-cellular carbon foams. Finite Elem Anal Des 2007;44:45–52. http://dx.doi.org/10.1016/j.finel.2007.08.008.
[14] Pérez L, Lascano S, Aguilar C, Estay D, Messner U, Figueroa IA, et al. DEM-FEA estimation of pores arrangement effect on the compressive Young's modulus for Mg foams. Comput Mater Sci 2015;110:281–6. http://dx.doi.org/10.1016/j.commatsci.2015.08.042.
[15] Joshi UA, Joshi P, Harsha SP, Sharma SC. Evaluation of the mechanical properties of carbon nanotube based composites by finite element analysis. Int J Eng Sci Tech 2010;2(5):1098–107.
[16] Chawla N, Sidhu RS, Ganesh VV. Three-dimensional visualization and microstructure based modeling of deformation in particle-reinforced composites. Acta Mater 2005;54:1541–8. http://dx.doi.org/10.1016/j.actamat.2005.11.027.
[17] Gupta N, Pinisetty D, Shunmugasamy VC. Reinforced polymer matrix syntactic foams: effect of nano and micro-scale reinforcement. Springer Sci Bus Media 2013. http://dx.doi.org/10.1007/978-3-319-01243-8.
[18] Krommenhoek ML. Production of a novel aluminum-carbon nanotube composite open-cell foam Mechanical engineering M.Sc. degree Thesis. Faculty of San Diego State University, ProQuest Dissertations Publishing; 2015. 10020546.
[19] Frantziskonis G. Multiscale characterization of materials with distributed pores and inclusions and application to crack formation in an aluminum alloy. Probab Eng Mech 2002;17:359–67. http://dx.doi.org/10.1016/S0266-8920(02)00033-4.

[20] Frantziskonis G. Wavelet-based analysis of multiscale phenomena: application to material porosity and identification of dominant scales. Probab Eng Mech 2002;17:349–57. http://dx.doi.org/10.1016/S0266-8920(02)00032-2.
[21] Kloss C, Goniva C, Hager A, Amberger S, Pirker S. Models, algorithms and validation for opensource DEM and CFD–DEM. Prog Comput Fluid Dyn 2012;12:140–52. http://dx.doi.org/10.1504/PCFD.2012.047457.
[22] Zhang ZF, Zhang LC, Mai YW. Wear of ceramic particle-reinforced metal-matrix composites. Part II. A model of adhesive wear. J Mate Sci 1995;30:1967–71. http://dx.doi.org/10.1007/BF00353019.
[23] Yu N, Chang YW. Effects of CNT diameter on the uniaxial stress-strain behavior of CNT/Epoxy composites. J Nanomater 2008;2008:6. http://dx.doi.org/10.1155/2008/834248.
[24] Figueroa IA, Suarez MA, Velasco M, Pfeiffer H, Alcántar B, Gonzalez G, et al. Development of pure open-cell Mg foams as structured CO2 captor. Thermochim Acta 2015;621:74–80. http://dx.doi.org/10.1016/j.tca.2015.10.011.